JOURNAL OF MATERIALS SCIENCE 27 (1992) 569–579

Review
Diffusion bonding of ceramics

O. M. AKSELSEN
The Welding Centre, The Foundation for Scientific and Industrial Research, Norwegian Institute of Technology, N-7034 Trondheim, Norway

Diffusion bonding of ceramics to ceramics and to metals is reviewed, with primary emphasis on the effects of operational variables on joint strength. These include principal bonding parameters such as temperature, time and pressure. In addition, the influence of atmosphere, mismatch in coefficient of thermal expansion between the joint members, interlayers and surface structure are discussed. The mechanisms involved, i.e. plastic deformation, various forms of diffusion and power law creep, imply that temperature is the most important process parameter. Finally, a survey of variables employed in bonding of different ceramic–metal and ceramic–ceramic joints is included as a guideline for selection of materials and parameters.

1. Introduction

In general, ceramics are regarded as attractive materials for structural applications due to their excellent high-temperature properties, wear and corrosion resistance. However, the lack of adequate joining techniques has, in many cases, limited their use. Conventional fusion welding is normally not performed, with the exception of those methods which involve melting of very narrow regions (laser and electron beam welding). Hence, alternative techniques for joining of ceramics have been developed. In addition to adhesive bonding, these techniques include various types of brazing and solid state diffusion bonding.

The diffusion bonding of ceramics to ceramics and to metals is reviewed here, with primary emphasis on the effects of operational variables (temperature, time and pressure) on joint strength. A discussion of the influence of atmosphere, coefficient of thermal expansion, interlayers and surface structure is included. Finally, bonding parameters reported in literature are surveyed for various ceramic–ceramic and ceramic–metal joints.

2. Process advantages and disadvantages

In principle, diffusion bonding represents a group of joining techniques where strong bonds are achieved through solid state diffusion (without melting of base materials), e.g. diffusion welding or diffusion brazing. The latter one involves the use of melting filler metals (liquid-phase bonding), while interlayers for diffusion welding do not usually melt. The present paper deals mainly with diffusion welding. Although the components to be joined are subjected to both temperature and pressure, the bonding process only includes very small fractions of macroscopic deformation. A detailed discussion of various diffusion bonding techniques is contained in the literature [1–11].

Diffusion bonding is primarily employed in the joining of dissimilar materials, i.e. dissimilar metals, metal–glass, metal–ceramic and ceramic–glass, either directly or through the use of interlayers. In principle, four different types of joints can be obtained.

1. Identical materials.
2. Identical materials with a narrow interlayer which consists of another material.
3. Dissimilar materials.
4. Dissimilar materials with a narrow interlayer which consists of a third material.

Diffusion bonding may have several advantages compared with fusion welding. Some of these are given below [12].

1. Bond strength similar to that of the base metal.
2. Minimum distortion and deformation, and hence, accurate dimension control.
3. Thin and thick sections can be joined to each other.
4. Large surfaces can be more effectively joined compared with welding.
5. Cast, wrought and sintered powder products and dissimilar materials can be joined.
6. Diffusion bonding is probably the optimum technique for joining metal matrix composites (MMC).
7. Excellent corrosion resistance, because no fluxes are required.
8. Machining costs may be significantly reduced.

The process also involves lower temperature gradients than in fusion welding, and hence, less microstructural changes and lower residual stresses.

On the other hand, diffusion bonding requires a substantially longer joining time. In addition, the equipment costs are high due to the combination of high temperature and pressure in vacuum environments. This often limits the component dimensions, which may be unfavourable from an economical standpoint.

0022–2461/92 $03.00 + .12

3. Bonding mechanisms

It is now generally accepted that the mechanisms involved in diffusion bonding are analogous to those occurring in pressure sintering. These are [13, 14]: (1) plastic yielding resulting in deformation of original surface asperities, Fig. 1; (2) surface diffusion from a surface source to a neck; (3) volume diffusion from a surface source to a neck; (4) evaporation from a surface source to condensation at a neck; (5) grain-boundary diffusion from an interfacial source to a neck; (6) volume diffusion from an interfacial source to a neck; and (7) power law creep.

An illustration of the various routes of material transfer is contained in Fig. 2. These mechanisms are normally separated in two main stages.

Stage 1: plastic deformation. The contact area of asperities, though initially small, will rapidly grow until the applied load can be supported, which means that the local stress falls below the yield strength of the material.

Stage 2: diffusion and power law creep. The driving force for mechanisms 2–4 is the difference in surface curvature. Matter is transferred from the point of least curvature (sharp neck of the void at the bond interface) to the point of greatest curvature. Thus, as the voids change from an elliptical to a circular cross-section, the rates of these mechanisms will approach zero because the aspect ratio of the voids tends to unity.

In addition to these stages, recrystallization and grain growth may occur during bonding.

Several attempts have been made to model the mechanisms and processes involved in diffusion bonding [15–22]. However, these are all based on joining of similar material parts, primarily the titanium alloy Ti–6Al–4V [15–17, 20]. In addition, many of the models do not account for all mechanisms involved in the bonding process, e.g. the model of Hamilton [16],

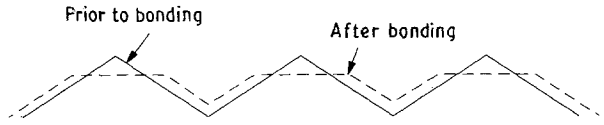

Figure 1 Reduction of surface roughness during initial stages of diffusion bonding, after Garmong *et al.* [17].

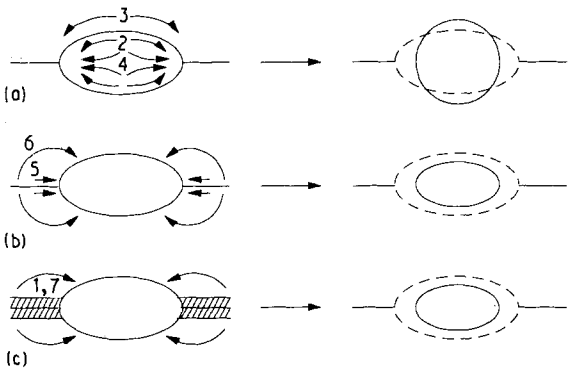

Figure 2 Schematic illustration of material transfer for various mechanisms involved in diffusion bonding: (a) surface source, (b) interface source, and (c) bulk deformation mechanisms, after Hill and Wallach [23].

which deals with the initial stages of bonding, considering plastic deformation only. Moreover, several simplifying assumptions have been made to solve diffusion equations, such as those inherent in the model of Allen and White [18]: no creep occurs; shrinkage of voids proceeds without change in their shape; grain-boundary diffusion occurs only along the bond plane; no contaminants (e.g. stable metal oxides) are present at the surface. Recent analysis has, however, shown that creep is important during the final bonding stages, as shown by Hill and Wallach when comparing predicted bonded length with experimental values obtained from metallographic examination [23]. The extent of creep, as well as that of grain-boundary diffusion, is dependent on the grain-growth behaviour at the bonding temperature. High-temperature creep is enhanced by grain refinement due to the rapid boundary diffusion of vacancies compared with that of bulk diffusion. Consequently, void shrinkage is favourably influenced by a reduction of the grain size adjacent to the bond plane.

The void geometry used in modelling diffusion bonding is important, because it determines the contribution from each operating mechanism. In contrast to the cylindrical geometry adopted by Allen and White [18], micrographs taken at various bonding stages [16, 17, 20] indicate that the void aspect ratio (height to length) is relatively low, and that the geometry is rather complex. In the recent model of Hill and Wallach [23], this situation has been taken into account by assuming an elliptical void geometry. Under such conditions, the dominating diffusion mechanism may shift depending on the instantaneous void aspect ratio. This means that the contribution from surface sources ceases when the aspect ratio approaches unity. When subsequent diffusion from interface sources changes the aspect ratio, surface diffusion may again become rate controlling. It follows that the model of Hill and Wallach seems to be the most accurate one published so far, and a brief summary of their model is, therefore, given below (reference is made to their paper for detailed derivation [23]).

The contribution from plastic yielding (Stage 1) to the fraction of bonded length, L_{yield}, was derived from an analysis by Johnson *et al.* [24]. Using von Mises' yield criterion, the following expression was obtained [23]:

$$L_{yield} = 3^{1/2}(Pb - \gamma)/2\sigma_y\left(1 + \frac{r_c}{L_{yield}}\right)\ln\left(1 + \frac{L_{yield}}{r_c}\right) \quad (1)$$

where P is the applied bonding pressure, σ_y the yield stress, γ the surface energy, b the width of the unit cell being modelled, and r_c the radius of curvature on the

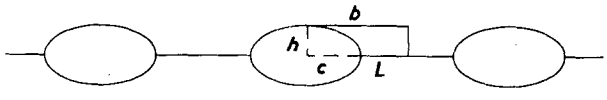

Figure 3 Definition of unit cell, after Hill and Wallach [23] (symbols are defined in the text).

major semi-axis of the ellipse. The unit cell is defined in Fig. 3.

In Stage 2, the contribution from mechanisms 2–4 (surface source) is represented by the following relationship (note that the bonding temperature is included in the calculation of Δh) [23]

$$\Delta L_i = \frac{\Delta h_i c}{h} \quad (2)$$

where ΔL is the rate of change in bonded length with time, Δh the rate of change in h with time, h is the height of the unit cell, c is the major semi-axis of the ellipse, and the subscript (i) represents the actual mechanism 2–4.

The fraction of bonded length resulting from interface sources is given by [23]

$$\Delta L_i = -\frac{\Delta h_i}{h}\left[b\left(\frac{4}{\pi} - 1\right) + l\right] \quad (3)$$

where l is the bonded length (equivalent to bonded area if unit thickness is considered) and b is the width of the unit cell.

In power law creep it is assumed that the ridge height decreases by the same amount as the void height, and that material is transferred to the void [23], resulting in a similar expression as Equation 3.

This model allows prediction of the bonded length versus temperature, time and external pressure, based on the assumption that the contribution from each operating mechanism can be added, i.e.

$$\text{bonded length: } L = L_{\text{yield}} + \sum_i \Delta L_i \quad (4)$$

In addition to the bonded length, the void volume (including change in volume with time) may be calculated for the respective mechanisms. An example of the resulting diffusion bonding diagram is shown for γ-iron in Fig. 4, with the dominant bonding mechanisms identified in each region. Although the predicted bonded length is close to measured values, a major problem in calculation would be the selection of representative values for activation energies, creep and diffusion constants. Such data are not readily available, and may limit the use of the model to a few metals and alloys.

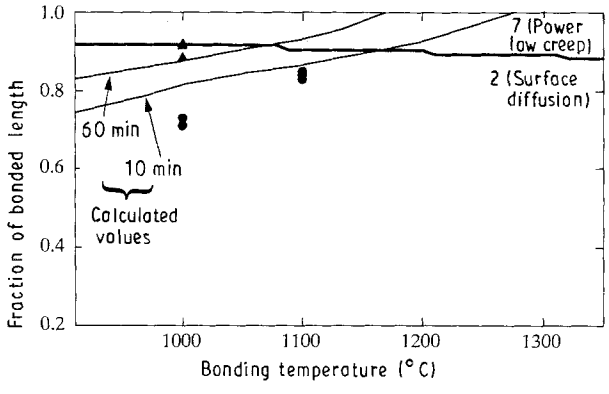

Figure 4 Prediction of bonded area in diffusion joining of γ-iron, applied bonding times of (●) 10 and (▲) 60 min, after Hill and Wallach [23] with experimental data from Derby and Wallach [22].

In the case of ceramic–metal joining, the lack of published data on the fraction of bonded length prevents a verification of the model for these materials. However, it would be expected that an extensive modification is required to account for the different chemical reactivity and thermal properties (e.g. coefficient of thermal expansion) between metals and ceramics. The bonding pressure will primarily result in plastic deformation of asperities of the metal only due to the rapid loss in strength at elevated temperatures. This means that the contacting process depends primarily on the deformation of the metal member. The formation of strong bonds will subsequently depend on void elimination. Thus, interdiffusion processes between the ceramic and the metal member are essential. Indications are that vacancy diffusion in ceramics is much slower than in metals. Finally, modelling of ceramic–metal joints should also include predictions of bond strength. It is not sufficient to estimate the fraction of bonded length due to the formation of high residual stresses as a result of the pertinent mismatch in the thermal expansion/contraction coefficient.

4. Effects of principal bonding parameters on joint strength

4.1. Temperature

The main process parameters in diffusion bonding are temperature, time and pressure. Temperature is, however, the most important one due to the fact that: (i) in thermally activated processes, a small change in temperature will result in the greatest change in process kinetics (diffusion, creep) compared with other parameters; and (ii) virtually all mechanisms in diffusion bonding are sensitive to temperature (plastic deformation, diffusion, creep). In general, the temperature required to obtain sufficient joint strength is typically within the range 0.5–0.8 of the absolute melting point of the base material. For metal–ceramic joints, bonding temperatures up to 90% of the metal melting point have been reported.

In diffusion bonding, sufficient strength is provided by elemental interdiffusion resulting in chemical reactions. Hence, the formation of a reaction zone will take place. The width of this zone, X, can be estimated from the following relationship with bonding temperature, T, and time, t:

$$X = K_p t^n = K_0 t^n \exp(-Q/RT) \quad (5)$$

where K_p is the penetration coefficient, K_0 represents a constant, n is the time exponent (usually close to 0.5), Q is an activation energy for diffusion and R is the gas constant. Note that the value of Q is dependent on the dominating diffusion mechanism, i.e. grain-boundary, lattice or surface diffusion. The rate of diffusion is normally increasing in the following order: lattice → boundary → surface. An example of such reaction zones is shown in Fig. 5 for a niobium–alumina joint.

The effect of temperature on the penetration coefficient is shown for SiC–Nb and SiC–Mo joints in Fig. 6. It is seen that the coefficient varies within large

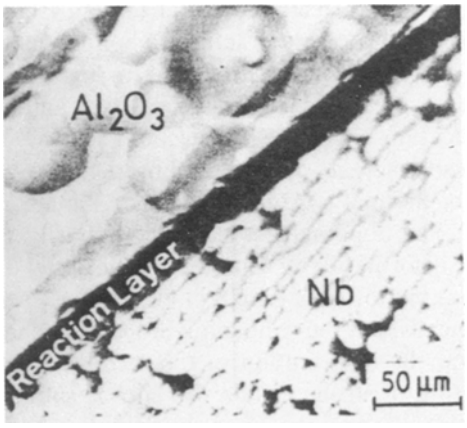

Figure 5 Reaction layer (NbO_x) in Al_2O_3–Nb joint, transmission electron micrograph after Morozumi *et al.* [25].

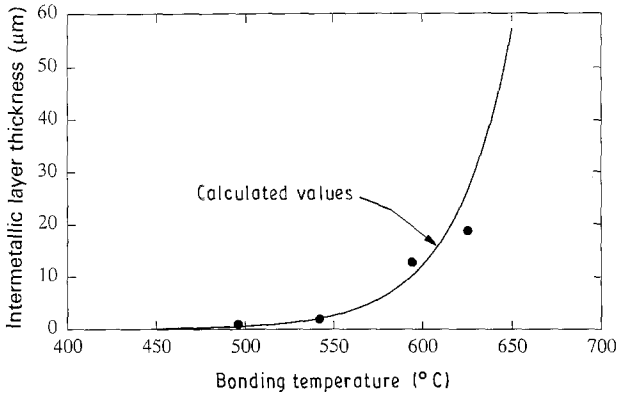

Figure 7 Effect of bonding temperature on thickness of reaction layer in joining of steel to alumina with 0.5 mm aluminium interlayer (vacuum, 30 min, 50 MPa). (●) Measured values, (———) calculated values from Equation 5, after Crispin and Nicholas [28].

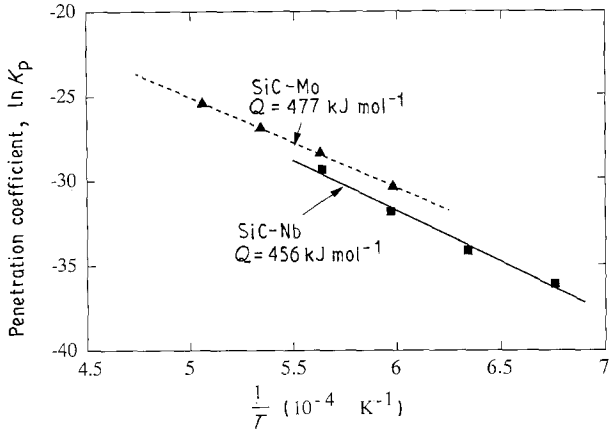

Figure 6 Effect of temperature on penetration coefficient in diffusion bonding (vacuum) of SiC to niobium, after Naka *et al.* [26] with additional data for SiC–Mo joints from Morozumi *et al.* [27].

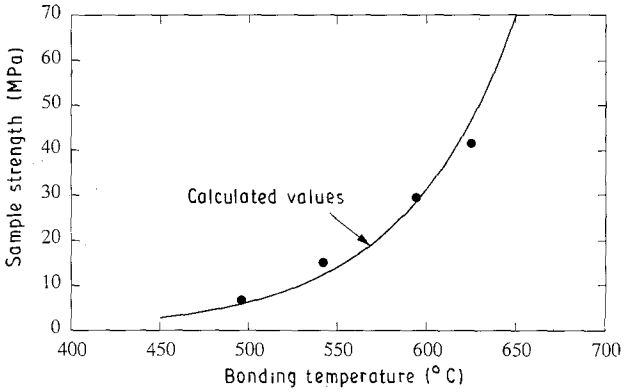

Figure 8 Effect of temperature on bond strength in joining of steel to alumina with 0.5 mm aluminium interlayer (vacuum, 30 min, 50 MPa). (●) Measured values, (———) calculated values from Equation 6, after Crispin and Nicholas [28].

limits, depending on the applied bonding temperature, e.g. from about 8×10^{-16} m^2 s^{-1} at 1470 K (1197 °C, 0.54 T_M of Nb) to 10^{-13} m^2 s^{-1} at 1750 K (1477 °C, 0.64 T_M of Nb) for SiC–Nb joints. In this case, the reaction layer shifts from Nb_5Si_3 to predominantly $NbSi_2$ when the temperature is raised from 1200 °C to 1400 °C. In addition to possible changes in the reaction layer chemical composition, its thickness will also increase with temperature, Equation 5. This is further evidenced by the data contained in Fig. 7 for steel–alumina joints with an aluminium interlayer (0.5 mm thickness) [28].

The corresponding effect of temperature on bond strength, BS, can be expressed by the following relationship, obtained on the basis of tensile testing [28, 29]

$$BS = B_0 \exp\left(-\frac{Q_{app}}{RT}\right) \quad (6)$$

where B_0 is a constant (MPa) and Q_{app} represents an apparent activation energy. It should be noted that Q_{app} can be regarded as a sum of activation energies, each representing the various factors contributing to the bond strength. As a consequence, the value of Q_{app} does not necessarily correspond to the value of Q in Equation 5.

The strength data for specimens with failure at the alumina–steel (aluminium interlayer) interface are presented graphically in Fig. 8. It is seen that the strength level increases with temperature, and that the calculated bond strength is in close agreement with the measured values. However, at higher bonding temperatures, it would be expected that the joint strength is reduced because of the high residual stresses formed as a result of thermal expansion mismatch between the joint members. The optimum bonding temperature occurs at a point where the strength reduction due to residual stresses starts to balance the strength enhancement as a result of void elimination. The presence of an optimum bonding temperature has been found in bend testing of silicon nitride–Invar joints with an aluminium interlayer [30].

In addition to these factors, the strength of ceramic–metal joints will also depend on the melting temperature of the metal. In fact, a linear increase in bond strength with increasing melting temperature has been found for metal–alumina joints [31] as shown in Fig. 9. This observation is not surprising, and may imply that the strength of ceramic–metal joints is related to the properties of the metal rather than those of the ceramic. The data presented in Fig. 9 are most useful for engineers who are involved in

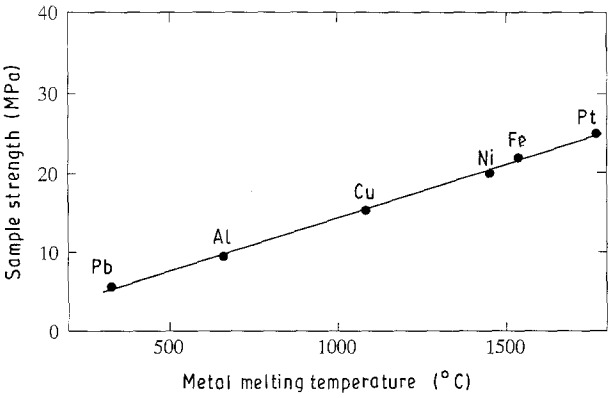

Figure 9 Effect of metal melting temperature on bond strength of metal–ceramic joints (bonding conditions depend on type of metal), after Klomp [32].

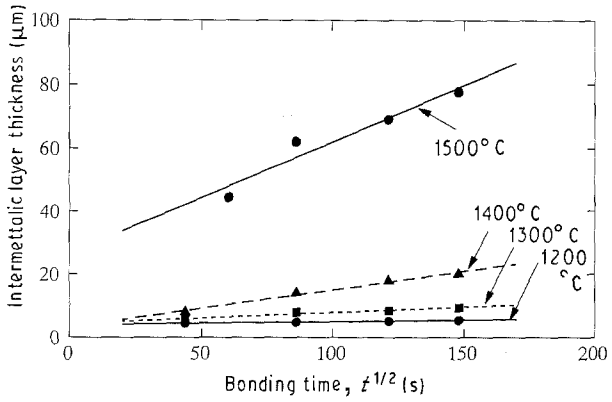

Figure 10 Effect of time on width of reaction zone in diffusion bonding of SiC–Nb joints (vacuum, 0.49 MPa pressure), after Naka *et al.* [26].

material selection. Combined with other data (e.g. corrosion, thermal expansion), Fig. 9 could form a basis for selecting materials where ceramic–metal joint strength is essential. Similar data for other ceramics are, therefore, highly needed.

4.2. Time

The effect of bonding time on reaction layer thickness can be roughly estimated from the following well-known expression:

$$X = k(Dt)^{1/2} \quad (7)$$

where k is a constant, D the diffusion coefficient and the time exponent n is equal to 0.5.

In many cases, the diffusion process may be dependent on the concentration of the diffusing element. Under such conditions, measured concentration profiles can be used to determine the value of D, i.e. Boltzmann–Matano analysis [33].

The effect of time on the width of the reaction zone has been plotted in Fig. 10 for SiC–Nb joints. It is apparent from the figure that the layer thickness follows a parabolic type of relationship with the bonding time ($n = 0.5$). Moreover, a similar time dependence has been obtained with respect to tensile strength, indicating that the strength can be expressed as follows [28]:

$$BS = B_0 t^{1/2} \quad (8)$$

where B_0 is a constant (MPa $s^{-1/2}$). An illustration of this point is contained in Fig. 11, based on tensile testing of Al_2O_3–Al joints. However, as experienced with temperature, an optimum bonding time would be expected to occur. This is confirmed by the data of Suganuma *et al.* [30] for Si_3N_4–Invar bonds with aluminium interlayers.

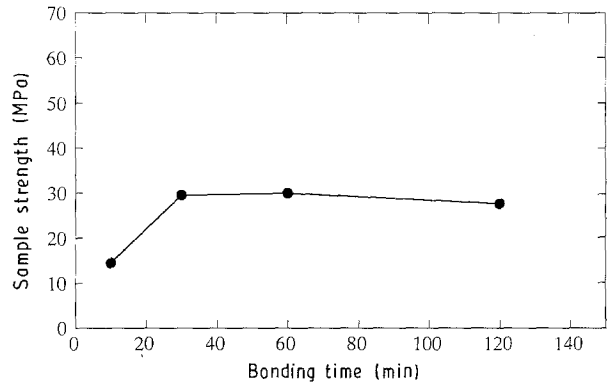

Figure 11 Effect of time on strength of diffusion-bonded (vacuum, 600 °C, 50 MPa) Al_2O_2–Al joints, after Crispin and Nicholas [28].

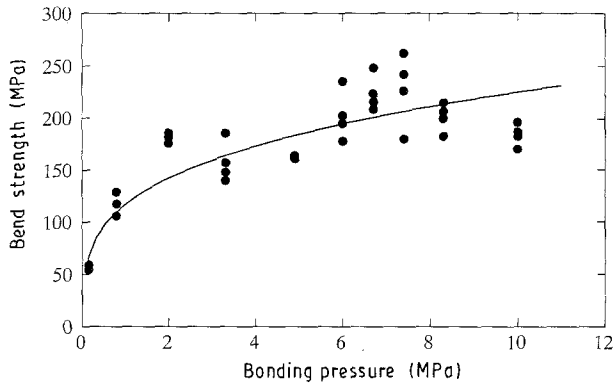

Figure 12 Effect of applied pressure on strength in diffusion bonding of Al_2O_3–Pt joints (air, 1450 °C, 240 min), after Allen and Borbidge [37].

4.3. Pressure

The pressure applied in diffusion bonding is typically some small fraction of the room-temperature yield stress to avoid macroscopic deformation, i.e. normally within the range 0–100 MPa. In general, this is sufficient to reduce the size of surface asperities and to provide oxide breakdown through plastic deformation at the bonding temperature. This, in turn, will increase the contact area subsequent to initial contact between the surfaces with a consequent reduction in the number of voids remaining from the initial stages of bonding. Similar to that experienced with temperature and time, indications are that an optimum pressure should be applied in order to obtain maximum joint strength [34, 35]. However, it is reasonable to assume that the effect of pressure is closely linked to the type of material being bonded, i.e. type and thickness of the oxide present at the surfaces. In the case of precious metals (Al_2O_3–Au and Al_2O_3–Pt joints) with

very narrow surface oxide layers, the strength increases with increasing external pressure up to a certain level, beyond which the strength becomes independent of pressure [36, 37]. This is shown for Al_2O_3–Pt joints in Fig. 12.

5. Chemical effects

5.1. Compound formation

In general, thermodynamic equilibrium considerations may be used to predict whether chemical bonds can be achieved under given experimental conditions (temperature, partial pressure of oxygen). Examples of possible macroscopic reactions during metal–ceramic joining under reducing atmosphere are [38]

$$Me_{I(s)} + 1/2O_{2(g)} \rightarrow Me_IO_{(s)} + \Delta G_1 \quad (9a)$$

$$Me_{II}O_{(s)} \rightarrow Me_{II(s)} + 1/2O_{2(g)} + \Delta G_2 \quad (9b)$$

$$Me_IO_{(s)} + Me_{II}O_{(s)} \rightarrow Me_IMe_{II}O_{2(s)} + \Delta G_3 \quad (9c)$$

$$Me_{I(s)} + Me_{II(s)} \rightarrow Me_IMe_{II(s)} + \Delta G_4 \quad (9d)$$

where ΔG_i is the free energy of the respective reactions.

In addition, the changes in surface tension (microscopic reactions) should be considered. As a result of removal of two surfaces, and formation of a new surface, the following energy balance was proposed [38]

$$A(\gamma_{cm} - \gamma_c - \gamma_m) + \Delta A\gamma_m = \Delta G_5 \quad (10)$$

where, γ_{cm}, γ_c and γ_m are the surface energy of the ceramic/metal, ceramic and metal, respectively, A represents the area of the ceramic/metal interface, and ΔA is the change in the metal surface area due to plastic deformation. The reaction will take place if $\sum_i^5 \Delta G_i < 0$. A similar approach can be made for non-oxide ceramics–metal joining (e.g. SiC and Si_3N_4).

Because many ceramics represent a state of high thermal stability and chemical inertness, the formation of strong bonds with metals requires elemental diffusion from the metal (or metallic interlayer) into the ceramic member. Under the prevailing circumstances (where the material surfaces are contaminated and possess a certain roughness), bonding will proceed far from the idealized conditions predicted theoretically by Equation 9. Moreover, the reaction kinetics may be too slow, thus preventing sufficient bonding for a given combination of temperature, time and pressure. Nevertheless, chemical reactions analogous to those described in Equation 9 have been reported. In the case of alumina, mixed oxides have been identified. Examples are $CuAlO_2$ [39, 40] and $NiO \cdot Al_2O_3$ (spinel type) [41] in Al_2O_3–Cu and Al_2O_3–Ni joints, respectively. Recent investigations have shown that formation of the spinel phase depends on the oxygen activity in nickel [41]. The overall chemical reaction is $Ni_{(s)} + \underline{O} + (1 + x_{max})\ Al_2O_3 = NiO \cdot (1 + x_{max})\ Al_2O_3$, $\Delta G^0 = -60.090 + 4.2T$ ($J\,mol^{-1}$) (where $\underline{\ }$ represents dissolved oxygen). Here x_{max} defines the Al_2O_3 saturated composition (quoted to be 0.38 at 1390 °C in [41]). This composition represents the first spinel formed due to the presence of excess Al_2O_3 during the initial stage. In the case of silicon carbide, intermetallic compounds of the type Nb_5Si_3 (γ phase), $NbSi_2$ (δ phase) [26] and Ni_2Si [42] (ε or δ, where ε represents the high-temperature form) have been found in SiC–Nb and SiC–Ni joints, respectively. In joining SiC to titanium, Ti_5Si_3 (ζ phase), Ti_3SiC_2 and TiC have been observed [43]. Here, the silicates represent the high-temperature form. Similar reactions would be expected to occur between silicon nitride and metals, with nitrides substituting carbides. The formation of these compounds presupposes that oxide films eventually present at the metal surface can be dissolved either through the use of a reducing atmosphere, or by applying load at the bonding temperature. As indicated above, the reaction layer may consist of several compounds, the composition being dependent on the actual bonding temperature. Consequently, the chemical reactions involved in bonding cannot be generalized, but should be determined in each individual case. Moreover, the rate-controlling mechanisms are not yet fully understood, which means that further work is required. In particular, diffusion data are still lacking for many alloys. In addition to chemical reactions, physical interactions are presumably operating. A brief discussion of these is contained in Reference 44.

5.2. Significance of bonding atmosphere

The formation of oxides during bonding implies that the partial pressure of oxygen is important to the joint mechanical properties. In most cases, it has been shown that vacuum bonding gives rise to superior joint strength compared with that of argon or air [28]. An example is shown for Si_3N_4–Si_3N_4 joints with aluminium interlayers in Fig. 13. In this case, vacuum bonding results in ductile fracture of the aluminium interlayer or brittle fracture within the ceramic. In contrast, bonding in air results in low joint strength caused by brittle fracture along the Al–Si_3N_4 interface, probably due to the presence of aluminium oxide [30]. This observation is in agreement with a higher partial pressure of oxygen. Although the bonding pressure has been sufficient for oxide breakdown, the formation of a new metal oxide layer may occur rapidly at a high partial pressure of oxygen, particularly when metals forming stable oxides are subjected to bonding.

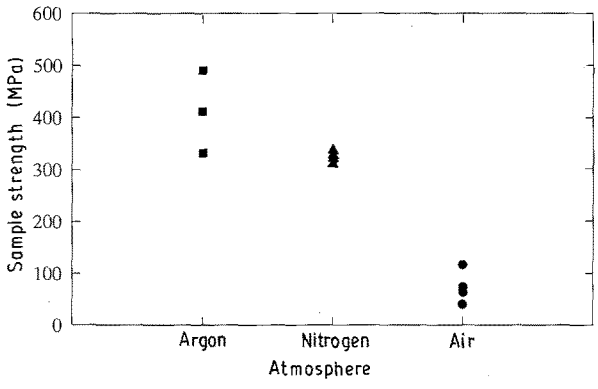

Figure 13 Effect of atmosphere on strength of Si_3N_4–Si_3N_4 joints with aluminium interlayer, after Suganuma *et al.* [30].

6. Effects of mismatch in coefficient of thermal expansion

6.1. Residual stresses

The residual stresses generated during bonding of ceramics to metals as a result of mismatch in thermal expansion/contraction between the joint members may be roughly estimated by the following expression [45] (fully elastic behaviour):

$$\sigma_i = -\sigma_j = \frac{E_i E_j}{E_i + E_j}(\alpha_i - \alpha_j)\Delta T \quad (11)$$

where E is Young's modulus, α the thermal expansion coefficient, ΔT the temperature cooling range, and i and j represent the materials being bonded.

Equation 11 predicts that the residual stresses increase with increasing thermal expansion mismatch and increasing bonding temperature. Because ceramics usually have a lower thermal expansion than metals, it would be expected that compression stresses exist within the ceramic body, and tensile stresses exist in the metal member. An exception may occur for metals with low thermal expansion such as possessed by many superalloys (e.g. Invar). It can readily be shown by inserting representative data in Equation 11 that very high residual stresses may develop on cooling from typical bonding temperature, and that the stress level may exceed the yield point of the metal resulting in plastic deformation.

In practice, however, the stress distribution in ceramic–metal joints will be more complex than that indicated by Equation 11 due to the application of a ductile interlayer. Moreover, the small specimen size frequently used to assess mechanical properties may introduce surface edge effects. A full treatment of the resulting elastic stresses under such conditions will not be included here. Reference is therefore made to the literature [46].

The effect of thermal expansion mismatch on bond strength is illustrated in Fig. 14 for Al_2O_3–metal joints with aluminium interlayers. It is seen from the Figure that the strength is monotonically reduced with increasing thermal expansion coefficient of the metal. This result is probably caused by an enhancement of the residual stresses with increasing mismatch in thermal expansion between the alumina and the metal. Thus, the higher strength level obtained in joining of Al_2O_3 to titanium and platinum is in agreement with the fact that their thermal expansion is close to that of alumina ($8 \times 10^{-6}\,°C^{-1}$). Similar trends have been reported for other ceramics such as SiC, Si_3N_4 and Sialon [47], although their lower coefficient of expansion ($\approx 4 \times 10^{-6}\,°C^{-1}$) requires some precaution in the metal selection. The low coefficient of thermal expansion of these materials makes them particularly attractive for applications such as advanced heat engines where resistance to thermal shock is important. As a consequence, they are frequently joined to superalloys such as Invar, Inconel or Nimonic because of the low mismatch in thermal expansion. However, the reactivity of silicon-based ceramics with some metals (e.g. titanium and nickel) at elevated temperatures [42, 48–51] may, as previously mentioned, give rise to the formation of silicides, silicates, nitrides and carbides, resulting in a substantial degradation of the high-temperature properties.

6.2. Interlayers

The use of interlayers in diffusion bonding is required for many applications in order to reduce bonding temperature, bonding pressure and bonding time, to enhance diffusion, and scavenge impurity elements. Although these factors are essential, the primary need for applying ductile interlayers is to reduce the residual stresses generated at the bond interface. This reduction is very important in high-temperature service behaviour of ceramics. When the joint is subjected to thermal cycling or thermal shock, large stress concentrations may be introduced in parts of the ceramic. An illustration of the favourable effects of interlayers is contained in Fig. 15 for ferritic stainless steel–alumina joints. It is apparent from the figure that the residual stresses are reduced with increasing interlayer thickness. In this case, niobium is found to be most beneficial, because the coefficient of thermal expansion ($8.1 \times 10^{-6}\,m\,m^{-1}\,°C^{-1}$) is similar to that of alumina. However, it can be rationalized that the mechanical behaviour of joints is somewhat more complex, because the bond strength may be limited by plastic flow or ductile fracture of the metal if the reaction layer is

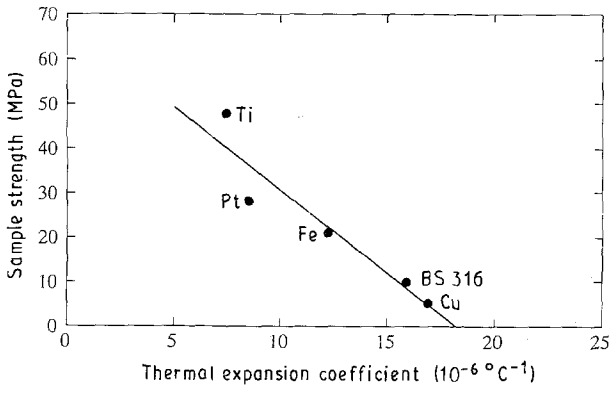

Figure 14 Effect of thermal expansion coefficient on sample strength level of Al_2O_3–metal joints with aluminium interlayers, after Crispin and Nicholas [28].

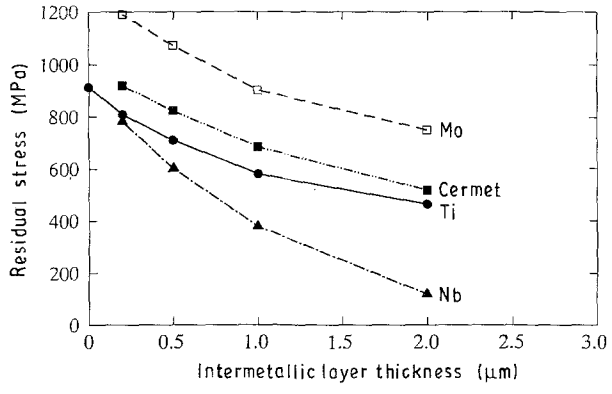

Figure 15 Effect of interlayer thickness on residual stresses of ferritic stainless steel (AISI 405)–alumina joints (1300 °C, 100 MPa, 30 min), after Suganuma *et al.* [52].

thick. In contrast, with a thin bond layer, failure may occur in the ceramic. Such observations have been made for Al_2O_3–Al and Al_2O_3–Al/4% Mg joints [53], as well as Al_2O_3–Ti joints [54]. Hence, the selection of interlayers is essential. A proper choice may prohibit partial melting at the bonding temperature, or the formation of eutectica with low melting point as a result of chemical reactions with the base metal. One approach to diffusion brazing is based on the formation of eutectica, and is well known from diffusion bonding of titanium to copper. This technique, also known as liquid-phase diffusion bonding, is described in the literature (e.g. [39, 54].) An improper selection may cause: deterioration of the joint properties at high temperatures through extensive chemical reactions, reduction of joint strength as a result of chemical reactions and high residual stresses, formation of unfavourable microstructures, and reduction of corrosion resistance. Interlayers can be applied in various forms such as powder or foils, or through metallization (e.g. thermal spray, galvanization, vapour phase deposition and hot isostatic pressing, HIP).

7. Surface structure

The joint strength may be significantly influenced by the roughness of the faying surfaces. This is normally not a problem for conventional metals and alloys. However, manufacturing and preparation of ceramic surfaces are regarded to be very difficult. Large surface roughness may introduce high local stress concentrations with subsequent initiation of brittle fracture. In joining techniques where melting filler metals are used (e.g. brazing), large roughness may cause severe problems and make it difficult to obtain the required wetting and spreading. An illustration of the effect of surface roughness on bond strength is contained in Fig. 16 for Si_3N_4–Al joints. It is seen from the figure that the strength is considerably reduced with increasing surface roughness, i.e. from 470 MPa to 270 MPa for a roughness of 0.1 and 0.3 μm, respectively. (Average surface roughness, R_a, has been used, R_a is defined as

$$R_a = (1/L)f(x)\,dx$$

where L is the measured length, $f(x)$ is the height of the surface measured from the centre line (ASME B46.1–1985).) This negative effect is probably linked to an increase in the size and number density of voids

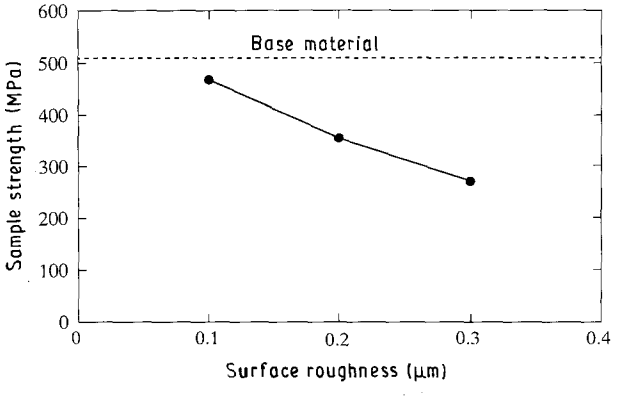

Figure 16 Effect of surface roughness on strength of Si_3N_4–Al joints (800 °C, 0.05 MPa, 10 min), after Suganuma *et al.* [55].

with increasing roughness. The strength level would be expected to increase when applying a higher bonding pressure and temperature. Moreover, the scatter in data (not included in Fig. 16) is substantially raised with increasing roughness. Under such conditions, a large number of tests is required to obtain sufficient data for a proper statistical evaluation of the results.

In addition to roughness, the microstructure adjacent to the bond plane is important. So far, very little work has been carried out within this field. In the previously described model by Hill and Wallach [23], a first assessment of the grain-orientation effects was included, because grain-boundary diffusion may depend on the angle between the applied pressure and a particular grain boundary. Their analysis was based on a statistical approach allowing several grain boundaries to be incorporated in the subsequent calculations. This seems to be reasonable, because it is likely that the volume of single voids is larger than the grain size during the initial stages of bonding. As a consequence, voids will be intersected by several grain boundaries. The resulting effect of grain size on bonded length was dependent on the material examined [23], although a reduction of the grain size tends to increase the rate of void elimination, and hence, increase the bonded length. This is in agreement with the fact that boundary diffusion is enhanced through grain refinement.

The significance of orientation of surface grains has also been discussed in joining of alumina to niobium [25] and copper [44]. In the former case, transmission electron microscopical examination of bonds showed that growth of NbO_x (Fig. 5), with a body centred tetragonal lattice, occurred epitaxially from the alumina grains, but with a rotation in the contact plane

$$[0\,0\,0\,1]_{Al_2O_3} \| [0\,1\,2]_{NbO_x}$$

$$[0\,\bar{3}\,3\,0]_{Al_2O_3} \| [\bar{1}\,\bar{2}\,1]_{NbO_x}$$

$$[\bar{2}\,1\,1\,0]_{Al_2O_3} \| [5\,\bar{2}\,1]_{NbO_x}$$

An interpretation of the resulting effect on the rate of bond formation has not yet been carried out, and the influence on joint strength remains to be assessed. However, growth of reactions products may introduce lattice mismatch and hence, residual stresses, suggesting that the reaction layer width should be narrow to provide sufficient bend strength. Further work is required to clarify the role of surface structure, including an examination of surface energy, γ, effects.

8. Survey of reported process variables

A large number of process parameters has been reported in the literature for various ceramic–metal and ceramic–ceramic joints. A representative selection of the material combinations examined is contained in Table I (additional data are available in the literature [61–68]). Included are operational variables such as temperature, time, pressure, atmosphere and type of interlayer. The resulting joint strength is also listed, together with the actual type of mechanical test carried out (i.e. bending, tensile and shear testing).

TABLE I Diffusion bonding parameters reported in the literature

Material combination	Temperature (°C)	Time (min)	Pressure (MPa)	Interlayer	Atm.	Strength[a] (MPa)	Reference
Al_2O_3–Ni	1350	20	100	–	H_2	200[b] (A)	[31, 32, 38]
Al_2O_3–Pt	1550	1.7–20	0.03–10	–	H_2	200–250 (A)	[31, 32, 38]
Al_2O_3–Al	600	1.7–5	7.5–15	–	H_2	95 (A)	[31, 32, 38]
Al_2O_3–Cu	1025–1050	155	1.5–5	–	H_2	153[b] (A)	[31, 32]
Al_2O_3–Cu_4Ti	800	20	50	–	Vac.	45[b] (T)	[56]
Al_2O_3–Fe	1375	1.7–6	0.7–10	–	H_2	220–231 (A)	[31, 32]
Al_2O_3–mild steel	1450	120	< 1	Co	Vac.	3–4 (S)	[38]
	1450	240	< 1	Ni	Vac.	0 (S)	[57]
Al_2O_3 high alloy steel	625	30	50	0.5 mm Al	Vac.	41.5[b] (T)	[29]
Al_2O_3–Cr	1100	15	120	–	Vac.	57–90[b] (S)	[35]
Al_2O_3–Pt–Al_2O_3	1650	240	0.8	–	Air	220 (A) See also Fig. 12	[37]
Si_3N_4–Invar	727–877	7	0–0.15	0.5 mm Al	Air	110–200 (A)	[30]
Si_3N_4–Nimonic 80A	1100	6–60	0–50	None,	Vac.	Details given in [58]	[58]
	1200			Cu, Ni, Kovar[c]			
Si_3N_4–Si_3N_4	770–986	10	0–0.15	10–20 μm Al	Air	320–490 (B)	[30]
Si_3N_4–Si_3N_4	1550	40–60	0–1.5	ZrO_2	Vac.	175 (B)	[59]
Si_3N_4–WC/Co	610	30	5	Al	Vac.	208[b] (A)	[47]
	610	30	5	Al–Si	Vac.	50[b] (A)	[47]
Si_3N_4–WC/Co	1050–1100	180–360	3–5	Fe–Ni–Cr	Vac.	> 90 (A)	[47]
SiC–Nb	1400	30	1.96	–	Vac.	87 (S) See also Fig. 10	[26]
SiC–Nimonic 80A							
	750–1000	60–168	15–100	None, Cu, Ni,	Vac.	Details given in [58]	[58]
	1000	168	100	Cu, Ni, Kovar[c]			
WC/Co–Cu, Co or Ni	1050–1400	60–1500	0.025–1	Cu, Co[d]	Vac.	Large scatter (A)	[60]
WC/Co–Al_2O_3	1300–1350	180	< 1	Ni	Vac.	2–4 (S)	[57]

[a] The letters in brackets represent the following test techniques. A, four-point bending; B, three-point bending; T, tensile testing; S, push-off shear testing.
[b] Maximum strength (optimum bonding conditions).
[c] Kovar: Fe–29%Ni–17%Co alloy.
[d] No interlayer in the case of WC/Co–Ni joints.

It should be noted that mechanical testing of ceramics may reveal a large scatter due to their brittle nature. The use of high-quality ceramics is required to obtain sufficient joint strength, which means that ceramic processing (e.g. reaction bonding, hot pressing) [59] and surface finish become very important. Moreover, assessment of mechanical properties with the test techniques reported in Table I may be insufficient to characterize fully joints made of dissimilar materials. Although four-point bending, in principle, should provide a reasonable constant stress level across the bond, inhomogeneous strain distribution may occur at the interface between the material members because of their different ability to undergo plastic deformation. In addition, surface cracks resulting from processing and preparation of ceramics may occasionally initiate brittle fracture, even in the absence of external load. Hence, it is reasonable to suggest that fracture toughness testing should be considered in order to examine the maximum allowable defect size in such joints. Extensive research initiated to improve the fracture toughness of ceramics is now in progress. It has already been shown that the cracking resistance may be improved by stabilization (transformation toughening). The mechanisms involved have been discussed in the literature [69]. A further enhancement of fracture toughness can be achieved through additions of, for example, silicon carbide whiskers or fibres (i.e. fibre-reinforced composites).

9. Conclusion

From the literature reviewed, it is obvious that diffusion bonding represents an attractive technique for joining ceramics to ceramics and to metals. At present, indications are that the bonding process is primarily dependent on the metal (or metallic interlayer), because the plastic deformation and diffusion stages within ceramics are relatively slow processes. Information on optimum process variables (temperature, time, pressure) is available in the literature for many ceramic–metal and ceramic–ceramic combinations, particularly for alumina, silicon carbide and silicon nitride, as well as tungsten carbide. Other ceramics such as titanium diboride (with very high initial hardness and strength) and stabilized zirconia still remain to be examined, although preliminary information on bonding of zirconia with nickel [70] or nickel oxide interlayer [71] is now available.

Computer modelling of joining ceramics to ceramics and to metals may provide a basis for the selection of operational parameters. At present, models developed for metals, predicting the fraction of bonded length, cannot be verified for dissimilar materials due to the lack of published data. In addition, predictions of bonded length are not sufficient for ceramics, because the residual stress formed during the bonding process may influence the bond strength considerably. Although diffusion bonding of ceramics has been thoroughly examined, there is a need for further work based on a more fundamental approach, with a few areas indicated in the text.

Acknowledgement

The author thanks the Norwegian Council for Technical and Scientific Research (NTNF) for financial support (Contract no. MT 3001.25312).

References

1. G. F. BLANK, *Mater. Des. Eng.* **64** (1966) 76.
2. R. F. TYLECOTE, *Weld. Met. Fabr.* **35** (1967) 483.
3. *Idem., ibid.* **36** (1968) 32.
4. *Idem., ibid.* **36** (1968) 67.
5. G. V. ALM, *Mater. Engng* **70** (1969) 24.
6. J. MORTIMER, *The Engineer* **231** (1970) 46.
7. A. G. METCALFE, *Amer. Mach./Metalworking Manufact.* **114** (1970) 97.
8. G. V. ALM, *Mech. Engng* **92** (1970) 24.
9. P. WIESNER, *Met. Constr. Brit. Weld. J.* (1971) 91.
10. P. M. BARTLE, *Weld. J.* **54** (1975) 799.
11. W. A. OWCZARSKI and D. F. PAULONIS, *ibid.* **60** (1981) 22.
12. P. G. PARTRIDGE, "Diffusion bonding of metals", AGARD (NATO), Aug. (1987) p. 5.1.
13. M. F. ASHBY, *Acta Metall.* **22** (1974) 275.
14. D. S. WILKINSON and M. F. ASHBY, *ibid.* **23** (1975) 1277.
15. W. H. KING and W. A. OWCZARSKI, *Weld. J.* **46** (1967) 289-s.
16. C. H. HAMILTON, in "Titanium Science and Technology", Vol. 1, edited by R. I. Jaffee and H. M. Burte (Plenum Press, New York, 1973) p. 625.
17. G. GARMONG, N. E. PATON and A. S. ARGON, *Metall. Trans.* **6A** (1975) 1269.
18. D. J. ALLEN and A. A. L. WHITE, in Proceedings of the Conference on "The Joining of Metal: Practice and Performance" Institute of Metallurgists (Warwick, 1981) p. 96.
19. B. DERBY and E. R. WALLACH, *Met. Sci.* **16** (1982) 49.
20. J. PILLING, D. W. LIVESEY, J. B. HAWKYARD and N. RIDLEY, *Met. Sci.* **18** (1984) 117.
21. B. DERBY and E. R. WALLACH, *Met. Sci.* **18** (1984) 427.
22. *Idem., J. Mater. Sci.* **19** (1984) 3140.
23. A. HILL and E. R. WALLACH, *Acta Metall.* **37** (1989) 2425.
24. W. JOHNSON, R. SOWERBY and R. D. VENTER, in "Plane Strain Slip Line Fields for Metal Deformation Processes" (Pergamon Press, Oxford, 1982) p. 119.
25. S. MOROZUMI, M. KIKUCHI and T. NISHINO, *J. Mater. Sci.* **16** (1981) 2137.
26. M. NAKA, T. SAITO and I. OKAMOTO, *Trans. JWRI* **17** (1988) 67.
27. S. MOROZUMI, M. KIKUCHI, S. SUGAI and M. HAYASHI, *J. Jpn Inst. Met.* **16** (1980) 1404.
28. R. M. CRISPIN and M. G. NICHOLAS, *J. Mater. Sci.* **17** (1982) 3347.
29. M. G. NICHOLAS and R. M. CRISPIN, *Proc. Brit. Ceram. Soc.* **32** (1982) 33.
30. K. SUGANUMA, T. OKAMOTO, M. KOIZUMI and M. SHIMADA, *J. Mater. Sci.* **22** (1987) 1359.
31. J. T. KLOMP, *Amer. Ceram. Soc. Bull.* **51** (1972) 683.
32. *Idem., Ceram. Sci.* **5** (1970) 501.
33. P. G. SHEWMON, "Diffusion in Solids" (McGraw-Hill, New York, 1963) p. 29.
34. C. A. CALOW, P. D. BAYER and I. T. PORTER, *J. Mater. Sci.* **6** (1971) 150.
35. C. A. CALOW and I. T. PORTER, *ibid.* (1971) 156.
36. F. P. BAILEY and K. J. T. BLACK, *ibid.* **13** (1978) 1045.
37. R. V. ALLEN and W. E. BORBIDGE, *ibid.* **18** (1983) 2835.
38. J. T. KLOMP, *Amer. Ceram. Soc. Bull.* **59** (1980) 794.
39. C. BERAUD, M. COURBIERE, C. ESNOUF, D. JUVE and D. TREHEUX, *J. Mater. Sci.* **24** (1989) 4545.
40. M. COURBIERE, D. THREHEUX, C. BERAUD, C. ESNOUF, G. THOLLET and G. FANTOZZI, *J. de Phys.* **C1** (1986) 18.
41. K. P. TRUMBLE and M. RÜHLE, *Z. Metallkde* **81** (1990) 749.
42. M. R. JACKSON, R. L. MEHAN, A. M. DAVIS and E. L. HALL, *Metall. Trans.* **14A** (1983) 355.

43. S. K. CHOI, M. CHANDRASEKARAN and M. J. BRABERS, *J. Mater. Sci.* **25** (1990) 1957.
44. J. T. KLOMP, in "Fundamentals of diffusion bonding", edited by Ishida (Elsevier, 1987) p. 3.
45. X. S. NING, T. OKAMOTO, Y. MIYAMOTO, A. KOREEDA and K. SUGANUMA, *J. Mater. Sci.* **24** (1989) 2865.
46. M. TOYODA, T. KOMATSU, K. SATOH and M. NAYAMA, *Int. Inst. Weld.* Doc. X-1161-88 (1988).
47. T. YAMADA, A. KOHNO and S. HIOKI, in "Proceedings of the 2nd International Symposium on Ceramic Materials and Components for Engines", Lübeck-Travemunde, April 1986, p. 401. Edited by W. Bunk and H. Havsner (Deutch. Ker. Ges., Germany, 1986).
48. R. L. MEHAN and D. W. McKEE, *J. Mater. Sci.* **11** (1976) 1009.
49. R. L. MEHAN and R. B. BOLON, *ibid.* **14** (1979) 2471.
50. R. L. MEHAN and M. R. JACKSON, *Mater. Sci. Res.* **14** (1981) 513.
51. J. R. McDERMID, M. D. PUGH and R. A. L. DREW, *Metall. Ttans.* **20A** (1989) 1803.
52. K. SUGANUMA, T. OKAMOTO, M. KOIZUMI and M. SHIMADA, *J. Amer. Ceram. Soc. Commun.* **67** (1984) 256.
53. B. DALGLEISH, K. P. TRUMBLE and A. G. EVANS, *Acta Metall.* **37** (1989) 1923.
54. J. F. BURGESS, C. A. NEUGEBAUER and G. FLANAGAN, *J. Electrochem. Soc.* **122** (1975) 688.
55. K. SUGANUMA, T. OKAMOTO, M. KOIZUMI and M. SHIMADA, *Adv. Ceram. Mater.* **1** (1986) 356.
56. Y. ARATA, A. OHMORI, W. K. WLOSINSKI and S. SANO, *Trans. JWRI* **17** (1988) 73.
57. M. G. McGEE, *Proc. Brit. Ceram. Soc.* **34** (1984) 261.
58. T. YAMADA. H. SEKIGUCHI, H. OKAMOTO, S. AZUMA, A. KITAMURA and K. FUKAYA, *Nippon Kokan Tech. Rep. Overseas* **48** February (1987) 67.
59. P. F. BECHER and S. A. HALEN, *Amer. Ceram. Soc. Bull.* **58** (1979) 582.
60. A. M. COTTENDEN and E. A. ALMOND, *Met. Technol.* **8** (1981) 221.
61. H. J. de BRUIN, A. F. MOODIE and C. E. WARBLE, *J. Mater. Sci.* **7** (1972) 909.
62. A. F. MOODIE and C. E. WARBLE, *Phil. Mag.* **35** (1977) 201.
63. F. P. BAILEY and K. J. T. BLACK, *J. Mater. Sci.* **13** (1978) 1606.
64. G. ELSSNER, W. DIEM and J. S. WALLACE, *Mater. Sci. Res.* **14** (1981) 629.
65. E. A. ALMOND, A. M. COTTENDEN and M. G. McGEE, *Met. Sci. J.* **17** (1983) 153.
66. K. SUGANUMA, M. SHIMADA, T. OKAMOTO and M. KOIZUMI, *Proc. Brit. Ceram. Sci.* **34** (1984) 273.
67. R. M. CRISPIN and M. G. NICHOLAS, in "Proceedings of the International Conference on Joining of Ceramics, Glass and Metal", Vol. 1 (Fortsch. ber. Deut. Ker. Ges. Bad Nauheim, Germany, 1985) p. 212.
68. K. ATARASHIYA and R. NAGASAKI, in "Proceedings of the 5th International Conference on High Technology Joining", Brighton, UK, November 1987, Paper 14. BNF. Met. Technol. Centre for (Brazing and Soldering (BABS). (Wantage, Oxon, UK, 1987).
69. J. WANG and R. STEVENS, *J. Mater. Sci.* **24** (1989) 3421.
70. J. G. DUH and W. S. CHIEN, *ibid.* **25** (1990) 1529.
71. T. YAMANE, Y. MINAMINO, K. HIRAO and H. OHNISHI, *ibid.* **21** (1986) 4227.

Received 25 March
and accepted 24 April 1991